04

Characteristics of capacitive RF discharge in a magnetic field with a predominant radial component

© G.V. Shvydkiy, I.I. Zadiriev, K.V. Vavilin, E.A. Kralkina, A.M. Nikonov

Moscow State University, Moscow, Russia
e-mail: ekralkina@mail.ru

Received March 24, 2023
Revised May 16, 2023
Accepted May 22, 2023

The work presents the results of an experimental study of the characteristics of the RF capacitive discharge placed in a magnetic field with a predominant radial component. The experiments are performed in the plasma source, which has the geometry of a Hall thruster. The integrated characteristics of the discharge, as well as the axial distribution of the probe ion current in the channel of the plasma source, are measured using three diagrams of the organization of the external discharge circuit: with the open for DC discharge circuit, as well as in the combination of a capacitive discharge with a direct current discharge. The main measurements are made in the argon in the flowrate range of 0.75−1.8 mg/s and the power of the generator 80−300 W at a frequencies of 2, 4 and 13.56 MHz, the induction of the magnetic field lying in the range of 100−300 G. Evaluation of the parameters of the plasma engine based on capacitive RF discharge when working in air, argon and krypton are made.

Keywords: capacitive radio -frequency discharge, VAC, displacement current, active current.

DOI: 10.21883/0000000000

Introduction

One of the new urgent tasks facing the space industry is the organization of spacecraft flights in ultra-low earth orbits (~ 200 km) [1–4]. The presence of residual atmosphere at altitudes of about 200 km requires equipping the spacecraft with engines capable of long-term operation not only on inert gases, but also on their mixtures with air, and ideally — exclusively on air. A natural candidate for the operating process of such engines is a radio frequency (RF) discharge. One of the promising areas for using RF discharge in space engineering is to replace the working process of a Hall thruster (HT) based on a direct current discharge with a RF capacitive discharge (RFCD) [5–9]. The possibility of replacement is due to thefollowing facts: just as in a direct current discharge, in the RFCD near the electrodes jumps of quasi-stationary potential appear, which, in the presence of a quasi-radial magnetic field, should lead to the appearance of azimuthal drift of electrons and ion acceleration [7]. The possibility of direct current discharge (DCD) replacement with RFCD, as well as with a combination of DCD with RFCD in plasma sources with HT geometry, was considered earlier in papers [5–9]. It was shown that RFCD is easily ignited and burns in both inert and chemically active gases, without need in the presence of an electron-emitting cathode. The discharge properties significantly depend on the design of its external circuit. When using diagram of RFCD organization with open for DC electrodes, the latter can be moved outside the discharge gap, which minimizes the electrodes erosion due to the interaction of their material with chemically active particles. Besides, the flows of electrons and ions arriving at the electrodes are compensated in magnitude within the period of the RF field. This property of the discharge can make it possible to avoid the neutralizer use. However, as shown in [6,8], if RFCD circuit with open for DC electrodes is used, then it is impossible to obtain an ion flow with an energy exceeding 70 eV. A significant increase in ion energy can be achieved by closing for DC of electrodes, but in this case the flows of electrons and ions at the exit from the channel are uncompensated. The additional increase in energy and ion flow can be obtained by using the combination of RFCD with DCD [6]. Previously, all measurements presented in [5–9] were performed while working at a frequency of 13.56 MHz. In this paper the discharge parameters in a plasma source with HT geometry are studied with changes in the operating frequency and induction of the external magnetic field.

1. Experimental diagram and procedure

In the experimental studies a plasma source was used, it was made in the geometry of Hall thruster (HT) with a diameter of 70 mm. The diagram of organization of the magnetic conductors and coils remained unchanged, with the exception of disconnecting the magnet coils from the discharge circuit and connecting them to an external power source. The laboratory ion source was mounted on the flange of a vacuum chamber with a volume of about 0.8 m^3, while the source housing was grounded. The vacuum chamber was evacuated by a cascade of two pumps — forevacuum and turbomolecular to a pressure of $3 \cdot 10^{-5}$ Torr; during the discharge burning the pressure varied in the range from $8 \cdot 10^{-4}$ to $3 \cdot 10^{-3}$ Torr depending on the experimental conditions. The main working gas

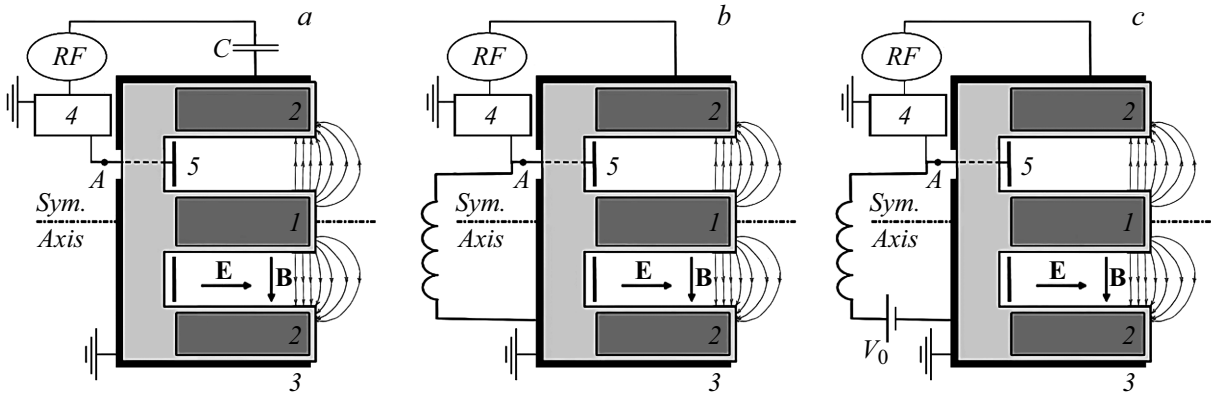

Figure 1. RFCD connection diagrams: *a* — with isolation capacitor, *b* — with closing for DC, *c* — combination of capacitive discharge with direct current discharge. *1, 2* — internal and external magnet coils, *3* — grounded housing, *4* — matching system, *5* — loaded electrode, *C* — isolation capacitance.

was argon, but a number of experiments were carried out with krypton and air. The active electrode, located deep in the channel at the site of the anode in the standard HT circuit, was connected to an external RF generator through a matching system in three ways: with opening for DC circuit , with closed for DC circuit, and with the supply of additional constant voltage to the loaded electrode. The third method is a combination of RFCD and direct current discharge (DCD). The corresponding diagrams are presented in Fig. 1. In the first case, the active and grounded electrodes were separated by direct current using isolation capacitance C equal to 1500 pF. To implement the second connection method, a choke — spiral with high inductance, was connected between the electrodes, this allowed direct current flow. For the third circuit a constant voltage source was connected in series to the external circuit, i.e. a combined RFCD and DCD was used. RF generators with a frequency of 2, 4 and 13.56 MHz were used, the range of powers considered was 90−300 W. In most cases, the reflected power of the RF generator did not exceed 15 W. In this paper, the current-voltage curves (CVCs) of the discharge were studied. The RF voltage between the active electrode and ground was measured using a Tektronix TDS 1012B two-channel oscilloscope and a capacitive divider. The discharge current was measured using a Rogowski coil [10], which was located between the active electrode and the matching system. Before starting the experiments, the Rogowski coil was calibrated for each operating frequency considered. The oscilloscope readings were averaged over 64 measurements, which significantly reduced the random error. In this regard, the main inaccuracy in the measurements was introduced by systematic errors, namely the inaccuracy in determining the divider coefficient, the calibration coefficient of the Rogowski coil and the influence of parasitic capacitances. In a diagram with open electrodes, the constant displacement of the loaded electrode was measured. To do this, a resistive divider with a division ratio of 1/500 was connected to the loaded electrode. The signal from the divider was fed to the oscilloscope channel, with the help of which the constant component of voltage was determined. In a circuit with closed electrodes, it becomes possible to measure the current flowing between the active electrode and the ground. In order to measure it, an analog ammeter was connected in series to the discharge circuit. To study the ion energy at the exit from the plasma source, a four-grid energy analyzer [8,11] was used. The energy analyzer was located in a vacuum chamber directly opposite the discharge channel at a distance of 20 cm from it. At this distance the current to the collector was large enough to distinguish it on noise background, but the energy analyzer was far enough away so as not to disturb the discharge. The energy analyzer consists of four grids: the first grid was grounded so that the fields inside the meter did not go outside and affect the discharge, the second and fourth grids were under a slight negative voltage (~ -30 V) are for repulsion of external electrons and electrons caused by secondary ion-electron emission from the collector, and a positive ion-retaining potential was applied to the third grid from a constant voltage source in the range 0−500 V. The average energy of the ion flow was determined based on the curve obtained by differentiating the collector current by the retarding voltage. To determine the ion saturation current along the discharge channel a Langmuir cylindrical probe with a diameter of 0.3 mm and 4 mm long was used, located on a movable carriage, which made it possible to move the probe along the channel. A standard probe electrical circuit was used. To increase the circuit impedance at the fundamental frequency and the second harmonic, two bandpass filters consisting of LC-sections were connected in series with the probe. The voltage supplied to the probe was measured on the first channel of the oscilloscope through the voltage divider, and to determine the ion current a resistance of a known value was used, the voltage drop across which was measured on the second channel of the oscilloscope. A large capacitance was connected in parallel to the resistance in order to reduce the amount of RF noise. The experiments were carried out under the

following conditions: the supplied power of RF generator was 90–300 W, the operating frequencies of the generator were — 2, 4 and 13.56 MHz. Working gases — argon (flow rate 0.75–1.8 mg/s), krypton (1.6 mg/s), air (1.5 mg/s). The magnitude of the magnetic field in all experiments was the same and amounted to 210 G. The magnitude of the constant voltage varied in the range 0–300 V.

2. Experimental results

2.1. Discharge CVC

Experiments showed that when the first discharge circuit with open for DC electrodes is used, the time dependence of voltage $U_{\mathrm{RF}}(t)$ and current $I_{\mathrm{RF}}(t)$ is harmonic with a good degree of accuracy. If the second and third diagrams of organization of discharge are used, when the electrodes are closed for DC the dependences $U_{\mathrm{RF}}(t)$, $I_{\mathrm{RF}}(t)$ are more complex. Fourier analysis showed that the spectrum $I_{\mathrm{RF}}(t)$ contains the first, second and third harmonics, the last of which is less than 10% of the first, while voltage is mainly represented by the first and to a lesser extent (50% of the first) by third harmonic. Further, to consider CVC the first harmonics of RF current and voltage, which make the greatest contribution to the absorption of RF power, were used. Fig. 2 shows the dependence of the amplitude of the first harmonic of the RF current on the amplitude of the RF voltage U_{RF} applied to the electrodes of the plasma source. The measurements were carried out when operating at frequency of 4 MHz using three discharge diagrams. To implement the discharge in a given power range of the RF generator, the highest values of RF voltage U_{RF} are required when using circuit with open for DC electrodes. The phase shift between RF current and voltage is close to -90 degrees, indicating the overwhelming contribution of the bias current to I_{RF}. In case of closed for DC electrodes, the discharge burning voltage decreases, and the RF current increases. Thus, the amplitude voltage values are in the range 400–500 V, and the current values are in the range 0.3–1.1 A. The increase I_{RF} with power increasing of the RF generator occurs at almost constant voltage between the electrodes, similar to what happens in the direct current discharge during its normal burning mode. The phase shift $\delta\varphi$ between $U_{\mathrm{RF}}(t)$ and $I_{\mathrm{RF}}(t)$ lies in the range -40–$30°$, which is significantly higher than in the case if the first diagram is used. Thus, when moving to the diagram with closed for DC electrodes, the proportion of the displacement current decreases, and the proportion of the conduction current in the total current increases.

When a potential that is positive relative to ground is applied using a DC power source (Fig. 1, *c*) to the loaded electrode, a significant drop in the work voltage and increase in the RF current are observed. It comes under notice that the phase shift between the RF current and voltage is close to 30°. In the paper [12] it was shown that when potential negative relative to ground is applied to the loaded electrode, CVC of the discharge occupies an intermediate

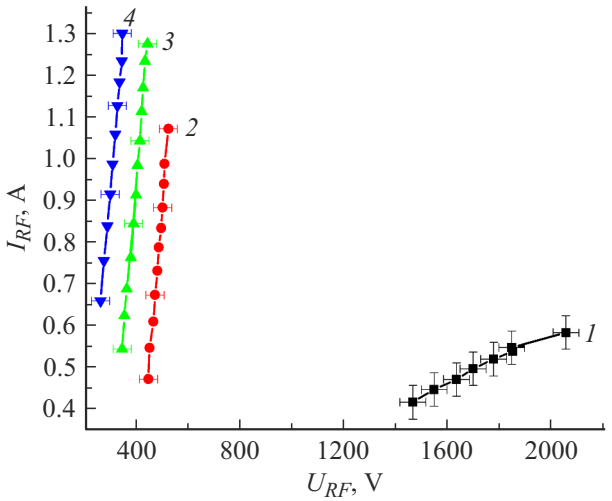

Figure 2. CVC of discharge for three discharge connection diagrams. $B = 210$ G. Work frequency — 4 MHz, gas — argon. *1* — open circuit, *2* — closed circuit, *3* — supply of constant voltage 100 V, *4* — supply of constant voltage 200 V.

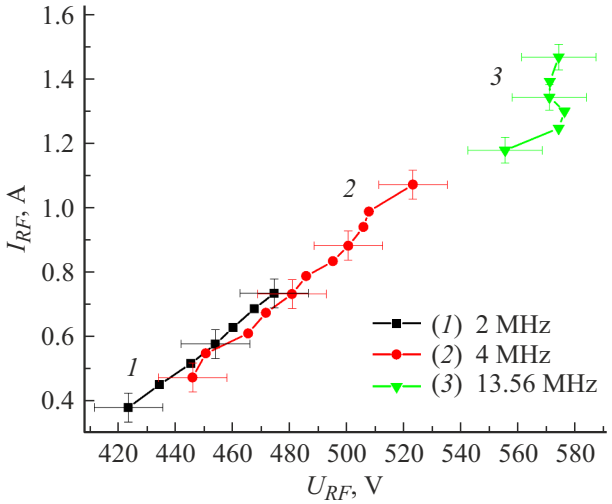

Figure 3. CVC of discharge for closed for DC electrodes. $B = 210$ G. Work frequency 2 (*1*), 4 (*2*), 13.56 MHz (*3*).

position between CVCs measured with open for DC and closed for DC electrodes.

Measurements performed at frequencies of 2 and 13.56 MHz [12] showed that the qualitative dependence of the discharge current-voltage characteristic on its organization scheme is similar to that obtained at $f = 4$ MHz. Let us consider in more detail the dependences $I_{\mathrm{RF}}(U_{\mathrm{RF}})$, measured when operating at frequencies of 2, 4 and 13.56 MHz, circuit with closed for DC electrodes. The experimental results are presented in Fig. 3. Note that the nature of the dependence $I_{\mathrm{RF}}(U_{\mathrm{RF}})$, measured at $f = 2$, 4 MHz, differs from the nature of the curve for $f = 13.56$ MHz. If, when operating at frequency of 13.56 MHz, the shape of CVC is close to that observed in the normal

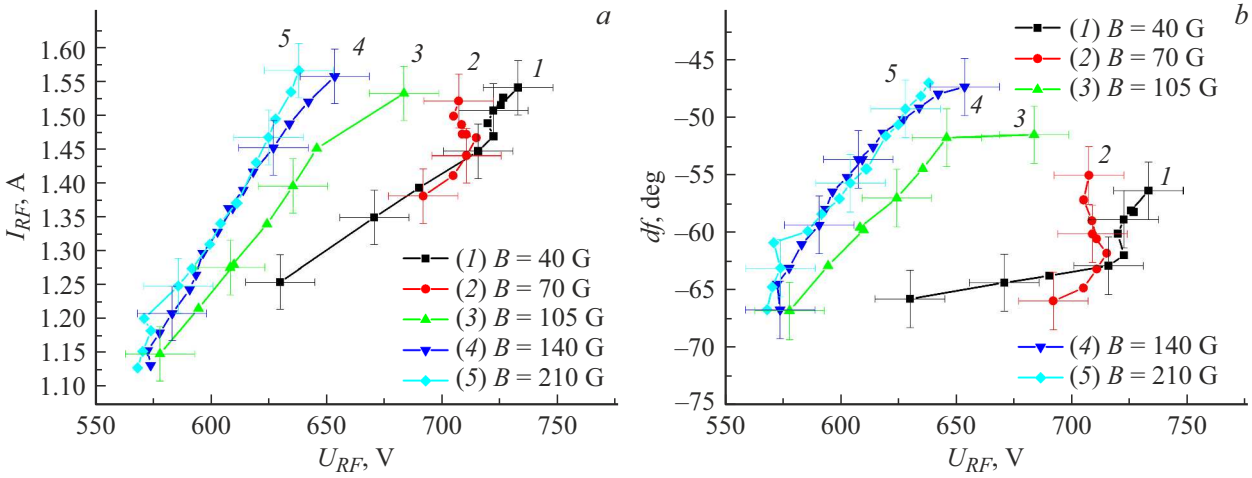

Figure 4. CVC of discharge (*a*) and phase shift between RF current and voltage (*b*) at different values of magnetic field induction. The case of close or DC electrodes. Operating frequency 13.56 MHz, gas — argon.

burning mode of the direct current discharge, then at lower frequencies the increase in the RF current requires increase in the RF voltage, which may indicate the implementation of a mode close to the anomalous burning mode of the glow discharge. As the operating frequency decreases, the absolute value of the phase shift decreases and approaches 20°, which indicates increase in the contribution of the conduction current to the total current I_{RF}. Recall that the present experiments at three frequencies considered were carried out in the same, fixed power range of the RF generator. In this case, increase in the active current is necessarily accompanied by a decrease in the discharge burning voltage U_{RF}, which was observed in the experiment. Let us further consider how the induction of an external magnetic field affects the shape of CVC. Fig. 4*a* shows the dependences of RF current amplitude I_{RF} on the voltage between the electrodes U_{RF} for the case of closed for DC electrodes. It can be seen from the Figure that at small values of B the discharge is ignited in α-mode. As U_{RF} increases, the discharge goes into γ-mode. In this case, the burning voltage first decreases, and a further increase in the current occurs with an increase in the RF voltage between the electrodes. At the same time, the phase difference begins to increase in the range — 70− − 55°, indicating increase in the role of the conduction current. Starting from $B = 105$ G, α-mode of the discharge is not observed at the considered powers of the RF generator, and the RF current increases sharply with increasing U_{RF} at all reviewed P_{gen}. Starting from $B = 140$ G, the values of I_{RF} weakly depend on the magnitude of the magnetic field.

2.2. Self-displacement of the loaded electrode and direct current flowing in external circuit

In the considered plasma source the RFCD is highly asymmetrical, since the area of the loaded electrode is significantly smaller than the area of the grounded electrode.

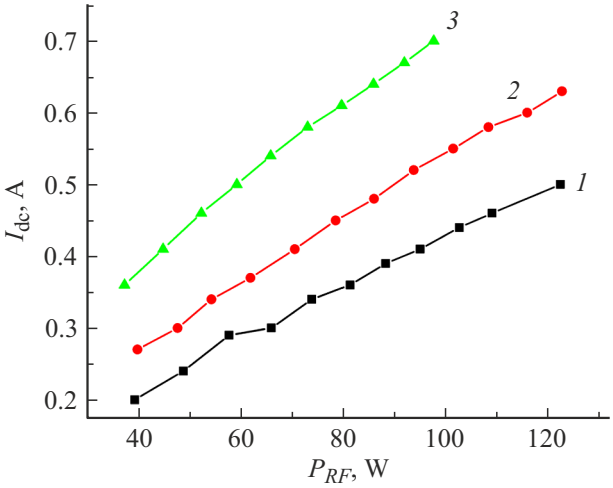

Figure 5. Direct current vs. input RF power for closed case at $V_{dx} = 0$ (*1*), 100 (*2*) and 200 V (*3*), $f = 4$ MHz.

As a consequence, in circuit with open for DC electrodes, the quasistationary potential drop in the layer near the loaded electrode significantly exceeds the potential drop in the layer near the grounded electrode [13–16], and a constant negative self-displacement of loaded electrode occurs U_a [8,13,14]. In these experiments the absolute value of U_a increased in proportion to the amplitude of the RF voltage, and when operating at frequency of 13.56 MHz, it changed in the range 600−740 V. When using the circuit with closed electrodes, the constant displacement of the active electrode disappears, and a constant current I_{dc} begins to flow in the external discharge circuit. Fig. 5 shows the dependences of I_{dc} on the power of the RF generator, measured using the second and third diagrams of organization of RFCD. Note that for greater clarity, the abscissa axis on the graph shows the power of the RF

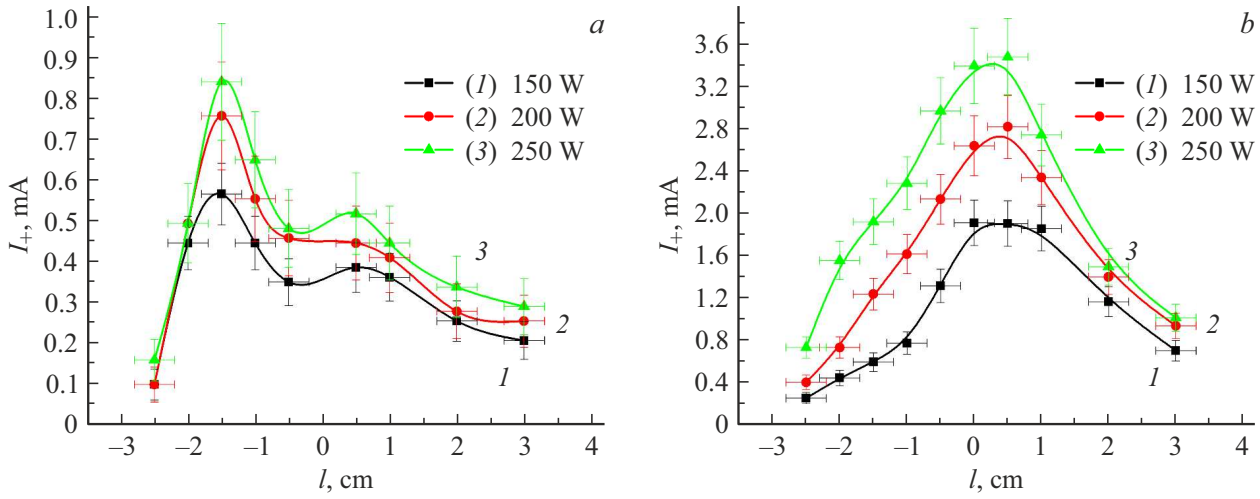

Figure 6. Distribution of ion saturation current along discharge channel for different powers of RF generator: *a* — open circuit, *b* — closed circuit. Generator frequency — 13.56 MHz, $B = 280$ G, gas — argon.

generator P_{RF}, and not RF voltage, since I_{dc} change occurs at an almost constant U_{RF}. As can be seen, with increase in the power of RF generator and the additional constant potential V_{dc} supplied to the loaded electrode, an increase in current I_{dc} is observed.

Measurements shown that increase in operating frequency is accompanied by a slight drop in the absolute value of direct current I_{dc}. Thus, when moving from frequency of 2 MHz to frequency of 13.56 MHz, on average, a drop in direct current of 60 mA is observed. For magnetic fields greater than 140Ġ at all operating frequencies considered, the absolute values of the current I_{dc} coincided within the limits of experimental errors.

2.3. Axial distribution of ion probe current in plasma source channel

Fig. 6 shows the distribution of the ion probe saturation current $i+$ along the discharge channel and in the jet of plasma flowing from it for closed and open circuits. When using a discharge circuit with open for DC electrodes (Fig 6, *a*) the dependence $i + (l)$ is non-monotonic, namely two maxima of ion current located near loaded electrode and the channel cut are observed. It is worth clarifying that the above errors are systematic and do not affect the relative location of the experimental points on the same curve. In case of closed for DC electrodes the nature of the distribution $i + (l)$ changes significantly (Fig. 6, *b*): the local maximum of the ion current at the loaded electrode disappears, and the maximum $i+$ in the channel end area increases significantly. Besides, the absolute values of the probe ion saturation current increase significantly. Experiments performed in [12] showed that the supply of V_{dc} to the loaded electrode is accompanied by an additional increase in the ion current near the channel end. Both when using the circuit with open for DC electrodes, and when they are closed, when power of RF generator increases, the values of $i + (l)$ increase throughout the entire measured area. The magnitude of the external radial magnetic field weakly affects the ion current distribution in the channel of the plasma source at $B > 140$ G. The obtained result correlates with the weak dependence of discharge CVC on B.

2.4. Ions energy

Previously, in papers [6,8] it was shown that the ion energy E when using circuit with open for DC electrodes does not exceed 70 eV. When using a circuit with closed electrodes, the ion energy increases significantly. Experiments showed that the maximum values are observed at operating frequency of 13.56 MHz, the minimum — when operating at frequency of 2 MHz. Thus, with increase in frequency from 2 to 13.56 MHz, the increase in E is about 100 eV. Also, increase in the positive displacement of the loaded electrode is accompanied by an increase in ion energy. The average ion energy weakly depends on the magnetic field induction: in the range 120–220 G it decreases by about 10%. This trend is associated with decrease in the amplitude of RF voltage U_{RF}, which, in turn, reduces the plasma potential and ion energy.

3. Characteristics of engine based on RF capacitive discharge with radial magnetic field

In order to get an idea of the prospects of use the plasma source operating on RFCD in HT geometry in the presence of radial magnetic field as rocket thruster, the average ion energy and direct current were measured for various work gases depending on the power of RF generator. The measurements were carried out with the second diagram of

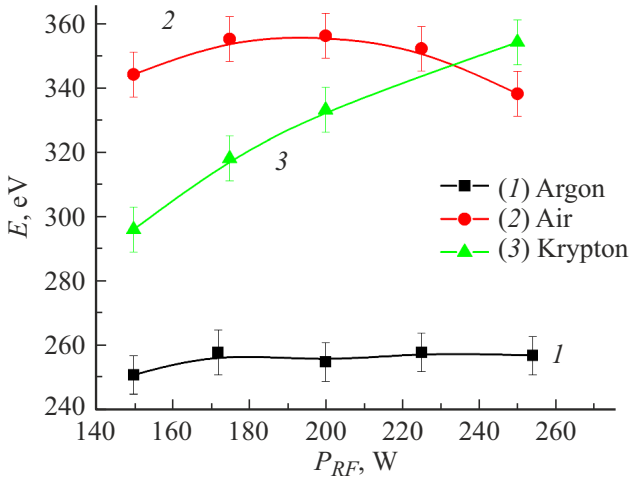

Figure 7. Average energy of ion beam vs. power of RF generator for work gases argon, krypton and air. Generator frequency — 1356 MHz, $B = 140$ G.

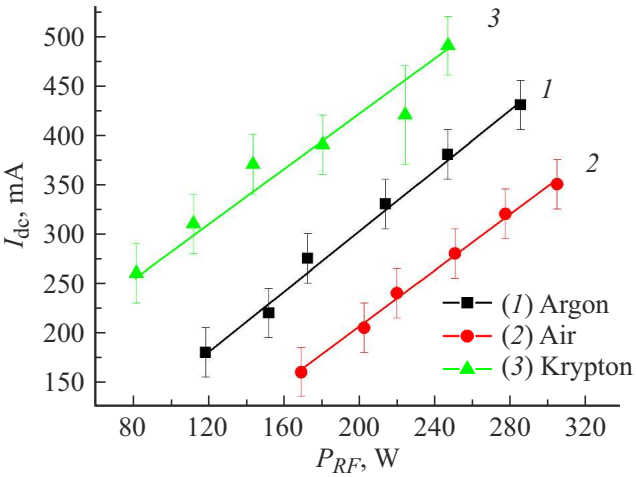

Figure 8. Direct current vs. power of RF generator for work gases argon, krypton and air. Generator frequency — 1356 MHz, $B = 140$ G.

organization of discharge. The obtained data on the average energy and density of ions in the jet flowing from the plasma source are presented in Figs 7 and 8. The maximum ion energy is achieved in the work gases (krypton and air) and is about 350 eV. Since the development of electric propulsion engines operating in air is currently underway, this result indicates the promising applicability of this source for flights in low Earth orbits. The maximum current was obtained with the work gas krypton, the minimum — with air. This result is quite natural and is explained by the difference in the potential and ionization cross section of the gas. In order to be able to compare the parameters of this source with existing electric propulsion engines, the following characteristics were calculated: the amount of power consumed to extract 1 A of ion current and the engine efficiency. It is worth noting that this is energy efficiency, but not traction efficiency, which is given in the electric propulsion engine passport. The traction efficiency is quite difficult to determine, since it is necessary to take into account the angular spread of the ions at the exit from the source. The considered characteristics are presented in the Table.

Characteristics of the RFCD engine for various working gases

Working gas	Air	Argon	Krypton
W/A	890	660	460
Energy, eV	350	255	350
Efficiency, %	37	38	65

4. Discussion of results

The physical properties of RFCD are largely determined by the patterns of formation of space charge layers near the electrodes. RFCD modification in diagram with isolation capacitance (Fig. 1, *a*) was well studied [13,14,17,18]. It is known that the main potential drop in the discharge is concentrated in the near-electrode layers of the spatial discharge. The discharge considered in this paper is highly asymmetrical, since the area of the loaded electrode is significantly lower than the area of the grounded electrode. As a consequence, in diagram open for DC electrodes the potential drop at the loaded electrode U_a, according to [13,14], shall significantly exceed the potential drop at the grounded electrode U_p, which is close to the floating potential. Previously performed experiments [9] showed that the potential difference between points lying in the channel region and at a distance of 4 cm from it is close to 75 V. The energy of the ions accelerated by this potential difference is 70 eV. Considering that the self-displacement of the active electrode under the experimental conditions is 600−700 V, we can assume that $U_a \sim 600-700$ V. A significant drop in potential at the loaded electrode leads to the ions acceleration in its direction and a significant removal of energy from the discharge. Accordingly, the fraction of the RF generator power used for ionizing atoms and heating electrons in the volume of the plasma source is small, which leads to a relatively low concentration of electrons in the discharge and low values of the conduction current. Knowing the potential drop and plasma parameters, it is possible to estimate the layer thickness at the loaded electrode, equating the values of the ion current flowing to the electrode, calculated using Bohm's formula, with the current calculated based on Child −Langmuir law [13]:

$$d_{sheath} = \left(\frac{1.86}{9\pi} \sqrt{\frac{2e}{M}} \frac{U_{sheath}^{\frac{3}{2}}}{en_+ v_+} \right)^{\frac{1}{2}},$$

where n_+ — ion density, $v_+ = 0.4\sqrt{\frac{2kT_e}{M}}$ — ion velocity, M — ion mass, d_{sheath} — layer thickness, U_{sheath} — potential drop in the layer. Estimates show that under the experimental conditions, the layer thickness did not exceed 0.6 cm, while the layer capacity was less than 4 pF. It is not surprising that the main contribution to the RF current flowing between the electrodes comes from the displacement current, which was observed experimentally. RF capacitive discharge with closed for DC electrodes is characterized by the so-called battery effect [13–15,19,20]. In any RF capacitive discharge within the period, the plasma changes its position - oscillates, alternately touching one or the other electrode. In the case when the electrodes are closed, and the area of the electrodes varies greatly (asymmetric discharge), the plasma never touches the electrode of a larger area. During the entire period the ion current flows to it, the current is proportional to the plasma density near the electrode. The electrode with a smaller area receives both ion current and electron current, which in excess compensates for the ion current at the moment of contact between the plasma and the electrode. I_{dc} flows in the external circuit from the electrode with larger area to the electrode with smaller area. Near the small electrode and in the plasma the current is carried by electrons, and near an electrode with larger area by ions. This means that the current I_{dc} is equal to the current of ions leaving the channel of the plasma source. Measurements of the plasma potential in the channel, as well as of the ion energy, show that the potential drop in the layer using diagram with closed for DC electrodes is about 250 V. Compared to the diagram with open for DC electrodes, the energy removal by ions decreases, the plasma concentration increases, the size of the near-electrode layers decreases, and the capacitance of the layers increases. This is accompanied by increase in the conduction current compared to the displacement current, which was recorded in the experiments performed. The third diagram of organization of discharge is a combination of RFCD and DCD. The RF channel is controlled by changing the power of the RF generator, and the DCD channel is controlled by changing the amount of displacement supplied to the loaded electrode. A positive displacement of the active electrode is accompanied by an increase in the plasma density in the channel, since additional power is supplied to the discharge from the direct current source. This leads to layer decreasing at the loaded electrode, an increase in the RF current flowing between the electrodes and its active part, as well as an additional increase of I_{dc}. Another consequence of DCD channel presence is its effect on the RF channel, which manifests itself in decrease in RF voltage applied to the electrodes at the same power of RF generator. The latter is the reason for the weak increase in ion energy with increasing in positive displacement of the loaded electrode. The energy of the ion beam increases as the operating frequency increases. In this case, each frequency is characterized by a weak dependence of the average ion energy on the power of the RF generator. The increase in ion energy with frequency increasing can be explained using the results of [14]. Estimates show that when operating at frequencies 2 and 4 MHz the generator frequency ω is less than the ion Langmuir frequency ω_{0i}. In this case, the impedance of the near-electrode layers is comparable to the plasma impedance, and part of the potential drops in the plasma region. As the frequency increases, the plasma impedance decreases, and most of the potential drops in the near-electrode layer, which increases the energy of the ion beam. The very weak dependence of the parameters of the plasma source on the magnetic field induction at B exceeding 140 G correlates with the weak dependence of the discharge parameters in the HT operating at direct current. When using the direct current discharge as operating process of HT, this effect is explained by the anomalous conductivity of the plasma [21–23]. The question of the mechanism of plasma conductivity when using RFCD as working process requires additional study.

Conclusion

In paper the experimental studies of characteristics of RFCD placed in magnetic field with a predominant radial component were carried out. The experiments are performed in the plasma source which has the geometry of Hall thruster. The integrated characteristics of the discharge, as well as the axial distribution of the probe ion saturation current in the channel of plasma source, are measured using three diagrams of organization of the external discharge circuit: with open and closed for DC electrodes, as well as in a combination of a capacitive discharge with a direct current discharge. The main measurements are made in argon in the flowrate range of $0.75-1.8$ mg/s and the power of RF generator $80-300$ W at frequencies of 2, 4 and 13.56 MHz, the induction of the magnetic field lying in the range of $100-300$ G. It is shown that when the diagram of organization of discharge changes, the operating range of RF currents and voltages changes, as well as the phase shift between them. The maximum RF voltage and current are observed in the discharge with the open for DC electrodes. When using diagram with closed for DC electrodes the discharge burning voltage and RF current are less than in open circuit, and the phase shift in absolute value decreases and approaches 0°. An increase in RF current with power increasing of the RF generator occurs at an almost constant RF voltage between the electrodes. Applying a constant displacement to the loaded electrode allows you to control the operating range of RF voltage and RF current. Also, a decrease in the operating frequency is accompanied by a shift in the operating range of RF voltages and currents to lower values. The external magnetic field with induction above 140 G has little effect on the operating range and values of RF voltages and currents and discharge impedance. The change in the diagram of organization of discharge is also accompanied by a significant rearrangement

of the axial distribution of local plasma parameters: in the diagram with open for DC electrodes, two maxima of the ion current are observed near the localization of quasi-stationary potential jumps. The main maximum of the ion current lies near the loaded electrode, where the main drop in the quasi-stationary potential is concentrated. Near the channel end, the maximum ion current is significantly lower; in diagram with closed electrodes the drop in the quasi-stationary potential at the grounded electrode increases, and the main maximum of the ion current shifts to the channel end region, where the radial magnetic field is localized. The average energy of ions in the plasma jet leaving plasma source depends significantly on the diagram of organization of discharge. In the case of open for DC electrodes and using argon as work gas it is 70 eV, and in the case of closed electrodes — 250 eV. The parameters of Hall thruster based on RF capacitive discharge were estimated when operating with air, argon and krypton.

Funding

This study was supported by grant of the Russian Science Foundation, project № 21-72-10090, https://rscf.ru/project/21-72-10090/.

Conflict of interest

The authors declare that they have no conflict of interest.

References

[1] A.S. Filatyev, O.V. Yanova. Acta Astronautica, **158**, 23 (2019). DOI: 10.1016/j.actaastro.2018.10.039
[2] F. Romano. RF Helicon Plasma Thruster for an Atmosphere-Breathing Electric Propulsion System (ABEP) (PhD thesis, 2021)
[3] P. Zheng, J. Wu, Yu Zhang, B. Wu. Intern. J. Aerospace Engineer., **2020**, 1 (2020). DOI: 10.1155/2020/8811847
[4] A.S. Filatyev, A.A. Golikov, A.I. Erofeev, S.A. Khartov, A.S. Lovtsov, D.I. Padalitsa, V.V. Skvortsov, O.V. Yanova. Progress in Aerospace Sciences, **136**, 100877 (2023). DOI: 10.1016/j.paerosci.2022.100877
[5] I.I. Zadiriev, E.A. Kralkina, K.V. Vavilin, G.V. Shvydkiy, A.F. Alexandrov. Prikladnaya fizika, **2**, 10 (2018) (in Russian).
[6] I.I. Zadiriev, E.A. Kralkina, K.V. Vavilin, G.V. Shvydkiy, A.F. Alexandrov. Prikladnaya fizika, **3**, 5 (2018) (in Russian).
[7] I.I. Zadiriev, E.A. Kralkina, K.V. Vavilin, G.V. Shvydkiy, A.F. Alexandrov. Prikladnaya fizika, **5**, 33 (2018) (in Russian).
[8] G.V. Shvydkiy, I.I. Zadiriev, E.A. Kralkina, K.V. Vavilin. Vacuum, **180**, 109588 (2020). DOI: 10.1016/j.vacuum.2020.109588
[9] G.V. Shvydkiy, I.I. Zadiriev, E.A. Kralkina, K.V. Vavilin. Plasma Physics Reports **47** (10), 1075(2021). DOI: 10.1134/S1063780X2110010X
[10] K.P. Manash, P.K. Chattopadhyay, D. Bora. Measurement Science and Technology, **18** (8), 2673 (2007).
[11] A.A. Shatalin, A.E. Kalinychev. Sbornik dokladov 16-j nauchno-tekhnicheskoj konferentsii „Molodezh v nauke". (Sarov, 2017), s. 351. (in Russian)
[12] G.V. Shvydkij. Teplofizika vysokikh temperatur. **1** (2023) (v pechati) (in Russian)
[13] Yu.P. Rajzer, M.N. Schnejder, N.A. Yatsenko. *Vysoko-chastotnyj emkostnoj razryad* (MFTI, M., 1995) (in Russian)
[14] V.P. Savinov. *Fizika vysoko-chastotnogo emkostnogo razryada* (Fizmalit, M., 2013) (in Russian)
[15] I.V. Schweigert, D.A. Ariskin, T.V. Chernoiziumskaya, A.S. Smirnov. Plasma Sources Sci. Technol., **20** (1), 015011 (2011). DOI: 10.1088/0963-0252/20/1/015011
[16] A. Diallo, S. Keller, Y. Shi, Y. Raitses, S. Mazouffre. Rev. Scientific Instrum., **86** (3), 033506 (2015). DOI: 10.1063/1.4914829
[17] M.A. Lieberman, A.J. Lichtenberg. *Principles of Plasma Discharges and Material Processing* (John Wiley & Sons Inc., Hoboken, 2005)
[18] P. Chabert. *Physics of Radio-Frequency Plasmas* (Cambridge University Press, 2011)
[19] J. Upadhyay, J. Peshl, S. Popović, A.-M. Valente-Feliciano, L. Vušković. AIP Adv., **8** (8), 085008 (2018). DOI: 10.1063/1.5045692
[20] M.D. Wiebold. *Dissertation Submitted in a Partial Fulfillment of Requirements for the Degree of Doctor of Philosophy* (Madison, University of Wisconsin, 2011)
[21] B.A. Jorns, S.E. Cusson, Z. Brown, E. Dale. Phys. Plasmas, **27** (2), 022311 (2020). DOI: 10.1063/1.5130680
[22] B. Jorns. Plasma Sources Sci. Technol., **27** (10), 104007 (2018). DOI: 10.1088/1361-6595/aae472
[23] A.I. Morozov, A.P. Shubin. Pisma v ZhTF, **10** (1), 28 (1984) (in Russian).

Translated by I.Mazurov